NJC

Carbon-TiO2 Hybrid Dots in Different Configurations – Optical Properties, Redox Characteristics, and Mechanistic Implications

SCHOLARONE™
Manuscripts

Please do not adjust margins

Journal Name

ARTICLE

Carbon-TiO₂ Hybrid Dots in Different Configurations – Optical Properties, Redox Characteristics, and Mechanistic Implications

Yamin Liu,[a] Yun Liu,[a] Haijun Qian,[a] Ping Wang,[a] Gregory E. LeCroy,[a] Christopher E. Bunker,[b,*] K. A. Shiral Fernando,[c] Liju Yang,[d,*] McIver Reibold,[a] Ya-Ping Sun[a,*]

Carbon-based hybrid nanostructures, especially carbon hybrid dots with metal oxides, are important to both fundamental studies and technological applications. In this work, carbon-TiO₂ hybrid dots in two different structural configurations were prepared and investigated comparatively for their optical properties and photoinduced redox characteristics, and the results suggested major differences. In the configuration of small carbon nanoparticles each coated/doped with only a small amount of TiO₂, the TiO₂ played the role of enhancing the surface passivation effect in conjunction with organic surface functionalization agents for the hybrid dots to exhibit much improved performance over that of their corresponding neat carbon dots. In the other configuration, however, the hybrid dots of TiO₂ nanocrystals each composited with nanoscale carbon domains were apparently similar to dye-sensitized TiO₂ nanoparticle systems, with the carbon domains serving the dye functions for the harvesting of visible photons. While combining nanoscale carbon and TiO₂ for various applications has been a popular topic in the recent literature, the results reported here provide new insights into the different structural configurations or arrangements between the carbon and TiO₂ and their associated effects on optical and photoinduced redox properties of the hybrid nanostructures. Significant implications of the results to an understanding of mechanistic relationships between the hybrid nano-structures/configurations and optical/redox properties are highlighted, and opportunities in the further exploration of carbon-metal oxide hybrid dots and their applications are discussed.

Introduction

Carbon "quantum" dots or carbon dots (CDots, Figure 1)[1-3] have attracted much recent attention for their interesting optical properties including especially the bright and colourful fluorescence emissions,[1,4,5] photoinduced redox characteristics and photocatalytic activities,[6-8] significant photodynamic effects,[9-11] and the related potential applications.[12-18] In fact, CDots now represent a rapidly advancing and expanding research field, as reflected by the large and ever increasing number of recent publications in the literature.[12-21]

In a general definition, CDots are small carbon nanoparticles with various surface passivation schemes (Figure 1). For the synthesis of CDots, the chemical functionalization of pre-processed and selected small carbon nanoparticles with organic molecules has been an effective method since the inception of this research field,[1] producing CDots of excellent fluorescence performance and related photoexcited state properties.[4,22,23] Such a synthesis, commonly referred to as the deliberate chemical functionalization method, yields CDots that should structurally adhere more closely to the general definition (Figure 1). However, even in CDots produced by the more popular carbonization synthesis, often in "one-pot" from a variety of organic precursors,[24-26] the general definition on CDots is still applicable such that in those dots on average the nanoscale carbon domains produced in the carbonization are passivated by organic species survived from the one-pot processing.[5] The same structural arrangements and understanding may be extended to carbon-based hybrid nanostructures (including those with the doping by nitrogen[20,21]), specifically hybrid dots of carbon and metal oxides, with similar passivation by organic species.[27-31] Among nanoscale metal oxides for the hybrid CDots, TiO₂ as a very well established semiconductor has been particularly popular.[32-34]
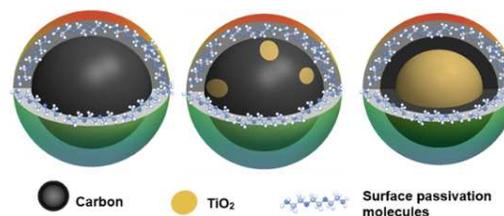
Figure 1. Cartoon illustrations on CDots (left), C_{TiO2}-Dots (middle), C/TiO₂-Dots (right)

[a] Department of Chemistry and Laboratory for Emerging Materials and Technology, Clemson University, Clemson, South Carolina 29634. E-mail: syaping@clemson.edu.
[b] Air Force Research Laboratory, Propulsion Directorate, Wright-Patterson Air Force Base, Ohio 45433. E-mail: christopher.bunker@wpafb.af.mil
[c] University of Dayton Research Institute, Sensors Technology Office, Dayton, Ohio 45469.
[d] Department of Pharmaceutical Sciences, Biomanufacturing Research Institute and Technology Enterprise, North Carolina Central University, Durham, NC 27707. Email: lyang@nccu.edu.

There may be different arrangements between the carbon and TiO_2 in a hybrid nanostructure, and also additional variations associated with the organic species for the passivation function, resulting in potentially dramatically different optical properties and redox characteristics. For example, small carbon nanoparticles could be surface-coated with a relatively small amount of TiO_2 and functionalized by organic molecules for hybrid CDots, denoted as C_{TiO2}-Dots (Figure 1).[22] These hybrid dots were found to be more fluorescent than their neat counterparts, and the observed high fluorescence quantum yields of the C_{TiO2}-Dots have been rationalized as being due to combined surface passivation effect on the core carbon nanoparticles by both the coated TiO_2 and the organic functionalization.[22]

In a different synthesis approach, hybrid dot structures of carbon with TiO_2 were prepared in carbonization processing of organic precursors in the presence of TiO_2 nanoparticles.[15,35-37] Among representative investigations, Vasei, et al. used emulsion polymerization of acrylonitrile around TiO_2 nanoparticles, followed by thermal carbonization of the resulting polyacrylonitrile for the desired structure of TiO_2 nanoparticles each with a carbon shell.[35] Wang, et al. prepared heterostructures of TiO_2 with carbon by using vitamin C as precursor for carbonization, and in their processing interactions between titanium ions in TiO_2 and hydroxyl groups in vitamin C were exploited for the anchoring of the precursor to the TiO_2 surface.[36] Since CDots have been demonstrated for their serving as relatively effective photocatalysts in some of the toughest energy conversation reactions, such as the visible light-driven photocatalytic CO_2 reduction and water-splitting,[7,8,38] there have been significant interests in the introduction of TiO_2 into CDots for potentially enhanced photocatalytic performance.[8,15] Xie, et al. used CDots to sensitize TiO_2 in composites for water-splitting under visible light irradiation, with the results suggesting significantly improved efficiencies.[39] Zhang, et al. combined CDots with TiO_2 nanorods by their assembly into microspheres for enhanced photocatalytic activities.[40] As a generalization, the carbon-TiO_2 hybrid dots of different compositions and configurations prepared by various carbonization processing protocols may be considered and denoted as C/TiO_2-Dots (Figure 1). The available experimental results suggest that the C/TiO_2-Dots may have significantly different excited state properties and processes not only from those of the C_{TiO2}-Dots (Figure 1), but also among themselves due to varying compositions and nanoscale configurations.

In this work, carbon-TiO_2 hybrid dots in structurally different configurations or arrangements between the carbon and TiO_2 domains in the core nanoparticles of the dots were prepared. These hybrid dots were characterized and evaluated for their optical and photoinduced redox properties, with their significant differences identified and discussed. Also discussed are mechanistic implications of the results and also issues on further development of the hybrid dots in reference to the dye-sensitized TiO_2 concept and systems already widely adopted in the literature.

Results and discussion

Carbon-TiO_2 hybrid dots in two rather different configurations were prepared for a comparative study of their optical and other properties. In one configuration denoted as C_{TiO2}-Dots (Figure 1), the carbon nanoparticle cores in CDots were coated (or more appropriately considered as "doped" because the carbon particle surface may not be entirely or even substantially covered) with only a small amount of TiO_2.[22] The other configuration, denoted as C/TiO_2-Dots (Figure 1), was obtained such that the pre-prepared and selected small TiO_2 nanoparticles were composited with

nanoscale carbon and functionalized by organic species in controlled carbonization reactions.

The C_{TiO2}-Dots were prepared by following the procedure reported previously.[22] Among key steps in the synthesis was the doping of pre-processed and selected small carbon nanoparticles with TiO_2. Briefly, a commercially acquired sample of carbon nanopowders was refluxed in aqueous nitric acid for purification and particle surface oxidation, coupled with dialysis to remove oxidized impurities. In the subsequent separation of the aqueous dispersed carbon nanoparticles by centrifugation, smaller nanoparticles retained in the supernatant were harvested. For the doping, a mixture of titanium ethoxide, ethanol, nitric acid, and water was prepared, and to the mixture were added the small carbon nanoparticles with sonication. Upon further sonication and then stirring for an extended period of time for the purpose of hydrolyzed titanium salts being deposited or adsorbed onto the carbon particle surface, the sample was annealed at 250 °C to obtain the TiO_2-doped carbon nanoparticles. The nanoparticles were then reacted in the melt of the oligomeric polyethylene glycol diamine (PEG_{1500N}),[22,41] and the reaction mixture was cleaned in a combination of centrifugation and dialysis to obtain the targeted C_{TiO2}-Dots in an aqueous solution. According to thermogravimetric analysis (TGA) coupled with inductively coupled plasma (ICP) quantification of Ti, the average TiO_2 content in the TiO_2-doped core carbon nanoparticles was 1-1.5 mol% in the C_{TiO2}-Dots.
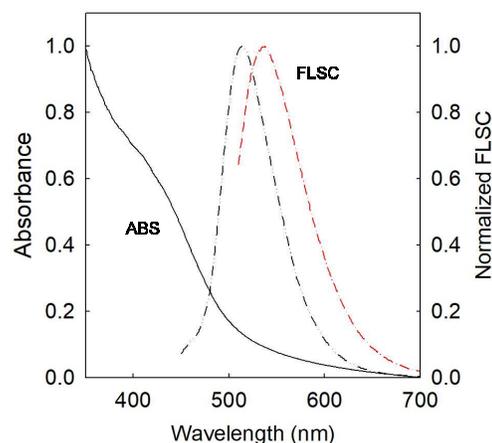

Figure 2. Absorption (ABS) and fluorescence (FLSC, with excitation at 440 nm: -..-..- and 500 nm: -.-.-) spectra of the C_{TiO2}-Dots in aqueous solution.

The UV/vis absorption spectrum of the C_{TiO2}-Dots is shown in Figure 2. The same as what was reported previously,[22] the spectrum exhibits an absorption shoulder around 430-440 nm. In the previous study,[22] the observation that the excitation into the absorption shoulder resulted in particularly bright fluorescence emissions in the green was rationalized as being due to special surface passivation effect by a combination of the doped TiO_2 and the organic species (the attached PEG_{1500N}). Since then, the special surface passivation effect has been found in some CDots without any doping by TiO_2 or other nanoscale semiconductors,[5,42] though these new results do not diminish the role of the doped TiO_2 in the C_{TiO2}-Dots to enhance the fluorescence performance. In fact, the fluorescence brightness was found to be dependent on the experimental conditions used in the doping of the small carbon nanoparticles with TiO_2, but an understanding

ARTICLE

toward the establishment of predictable correlations between the doping experiments and the fluorescence properties of the resulting C_{TiO2}-Dots still remains a challenge. The C_{TiO2}-Dots selected for spectroscopy investigations in this work had fluorescence quantum yields around 30% in the green (440 nm excitation). Also shown in Figure 2 are observed fluorescence spectra at two representative excitation wavelengths.

For the other configuration of the hybrid dots, C/TiO_2-Dots (Figure 1), small TiO_2 nanoparticles were prepared from titanium ethoxide in a hydrothermal processing, modified somewhat from what was reported in the literature.[43] Under the controlled processing conditions, the sample of TiO_2 nanoparticles with average sizes of 7.8±0.4 nm in diameter was obtained and used for further processing, where the particle sizes were estimated in terms of the Scherrer equation on the broadening in powder X-ray diffraction peaks (Figure 3).
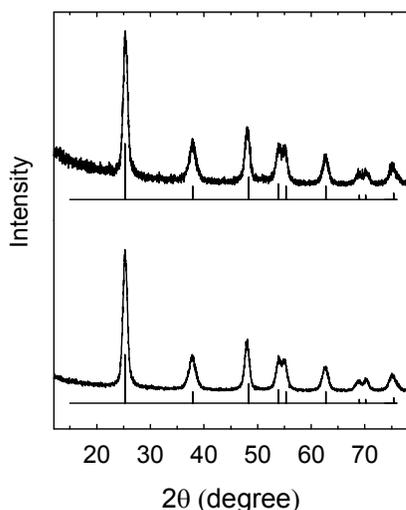

Figure 3. X-ray powder diffraction patterns of the TiO_2 nanoparticles (bottom) and the C/TiO_2-Dots with 71 wt% TiO_2 (upper), and their agreement with the standard diffraction pattern of anatase TiO_2.

The TiO_2 nanoparticles were dispersed in ethanol and mixed well with the oligomeric polyethylene glycol (average molecular weight ~1,500, PEG_{1500}) with sonication for an apparently homogeneous suspension. The carbonization processing was based on microwave irradiation, for which the rationale was such that the TiO_2 nanoparticles would preferentially absorb the microwave energy to become hot spots, thus facilitating the thermal carbonization of the surrounding PEG_{1500} species for the desired hybrid dot structures. The as-processed sample was cleaned via dialysis to yield the C/TiO_2-Dots in aqueous dispersion. The dispersion was solution-like and stable with respect to precipitation over an extended period of time (6 months or longer), generally different from what have been reported in the literature on carbon-TiO_2 composites,[36,39,40] thus enabling more quantitative investigations on their optical and related properties. By varying the PEG_{1500}/TiO_2 ratio in the precursor mixture and microwave processing conditions, two C/TiO_2-Dots samples with different TiO_2 contents of about 31 wt% (6.3 mol%) and 71 wt% (27 mol%) in the core nanoparticles of the dots (excluding the carbons in the surface PEG moieties) were prepared for characterization and subsequent investigations. For comparison, CDots in a similar configuration but without TiO_2, referred to as PEG-CDots, were prepared in the same microwave processing.

Powder X-ray diffraction results for the C/TiO_2-Dots show similar diffraction pattern and peak broadening to those of the TiO_2 nanoparticles (Figure 3), as expected. Since the microwave irradiation could in principle increase the crystallinity in the TiO_2 nanoparticles, the lack of changes in the peak broadening in the X-ray diffraction of the C/TiO_2-Dots may be explained such that the particles were already crystalline before the carbonization processing. The carbon domains in the C/TiO_2-Dots must be largely amorphous for the absence of any meaningful carbon-related diffraction peaks.

Transmission electron microscopy (TEM) images for the C/TiO_2-Dots (Figure 4) are apparently dominated by the TiO_2 nanoparticles for their much higher Z-contrast due to titanium. The average size and size distribution obtained from the TEM images of the TiO_2 nanoparticles (Figure 4) pretty much match those estimated from the peak broadening in the X-ray diffraction patterns (Figure 3). The well dispersion of the TiO_2 nanoparticles in the TEM images may imply that the C/TiO_2-Dots were similarly well dispersed. As the basis for the C/TiO_2-Dots, the co-localization of the TiO_2 nanoparticles and carbon domains is supported by the energy-disperse spectroscopy (EDS) mapping results (Figure 5).
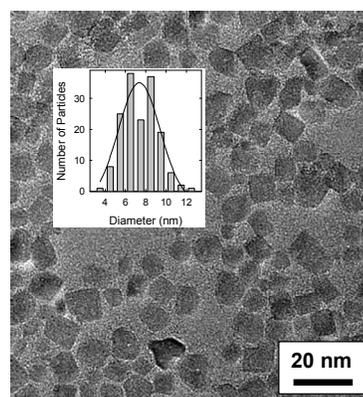

Figure 4. A representative TEM image of the C/TiO_2-Dots with 71 wt% TiO_2. Inset: A statistical analysis of the size distribution based on multiple TEM images of the sample.
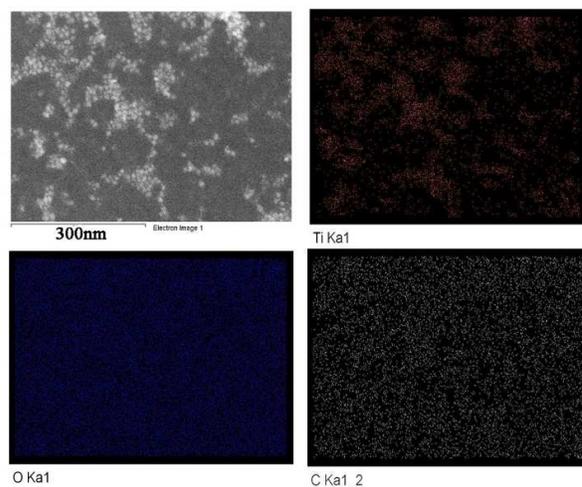

Figure 5. A TEM image in the Z-contrast mode (upper left) and the EDS mapping results on titanium (upper right), oxygen (lower left), and carbon (lower right) for the C/TiO_2-Dots with 71 wt% TiO_2.

FT-IR spectra of the hybrid dots are compared with those of the PEG-CDots and PEG$_{1500}$ molecules in Figure 6. For the two C/TiO$_2$-Dots samples, the broad peaks around 650-600 cm^{-1} may be assigned to Ti-O stretch vibrations, as similarly assigned in the literature,[44] and these peaks are mostly absent in the spectrum of the C$_{TiO2}$-Dots, consistent with the rather low TiO$_2$ content in the latter (less than 1.5 mol% in the core nanoparticles, as discussed above). It is interesting that all four dot samples exhibit absorption features in the carbonyl region around 1,700 cm^{-1} (Figure 6). For the C$_{TiO2}$-Dots, such features might not be surprising because the carbon nanoparticles used for the coating/doping by TiO$_2$ were surface oxidized in the treatment with nitric acid. However, the other three dot samples were prepared in the microwave-assisted thermal carbonization processing, so that the significant absorption features around 1,700 cm^{-1} might be considered as evidence for the formation of carbonyl moieties in the dot structure under the carbonization processing conditions.

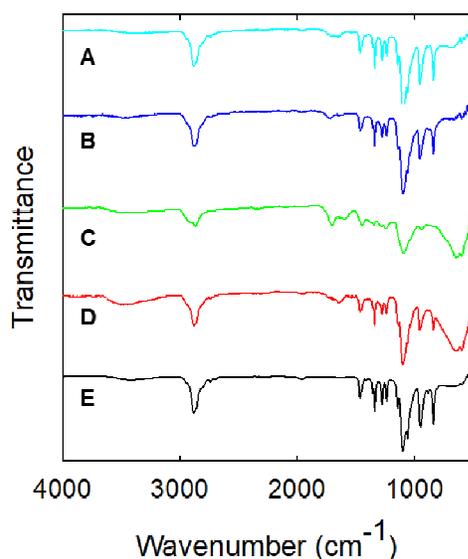Figure 6. FT-IR spectra of the C$_{TiO2}$-Dots (A), PEG-CDots (B), C/TiO$_2$-Dots with 31 wt% TiO$_2$ (C) and 71 wt% TiO$_2$ (D), and PEG$_{1500}$ (E).

Optical absorption spectra of the C/TiO$_2$-Dots (Figure 7) in the visible spectral region must be due to the carbon domains because the absorption small carbon nanoparticles (Figure 7). Between the two C/TiO$_2$-Dots samples, while their absorption spectral profiles were essentially the same, their cut-off of TiO$_2$ nanoparticles is in the UV. This was made more evident by the agreement of these absorption spectra with that of the aqueous dispersed small carbon nanoparticles (Figure 7). Between the two C/TiO$_2$-Dots samples, while their absorption spectral profiles were essentially the same, their absorbances were found to be proportionally different with respect to the carbon contents in the cores of the C/TiO$_2$-Dots.

Fluorescence emission spectra of the two C/TiO$_2$-Dots samples in aqueous solutions are also shown in Figure 7, which are both similar to the spectrum of the PEG-CDots. However, these carbon-TiO$_2$ hybrid dots are obviously less fluorescent than their neat counterpart, with observed quantum yields of about 1% for the C/TiO$_2$-Dots of 31 wt% TiO$_2$ and about 0.6% for the C/TiO$_2$-Dots of 71 wt% TiO$_2$ vs the yield of 3% for the PEG-CDots. The lower quantum yields in both C/TiO$_2$-Dots samples and the relatively even lower in the sample with more TiO$_2$ suggest the likely role of TiO$_2$ in the hybrid dots as quencher for the emissive excited states of the

carbon domains. In fact, the quenching should be expected because configuration-wise the C/TiO$_2$-Dots are equivalent to dye-sensitized semiconductors (TiO$_2$), with the carbon domains serving the dye function for photon-harvesting in the visible spectral region. What might be considered surprising is that the fluorescence emissions are not diminished even with the TiO$_2$ being in such close contact with the carbon domains in the hybrid dots. One explanation may be that the carbon domains are substantial in size, not a thin coating on the surface of the TiO$_2$ nanoparticles. By considering in a first approximation the hybrid dot structure as a sphere with a TiO$_2$ nanoparticle core (about 8 nm in diameter) and a carbon shell, the estimated shell thickness would be about 0.8 nm for the 71 wt% TiO$_2$ content and about 3 nm for the 31 wt% TiO$_2$ content in the C/TiO$_2$-Dots. In the actual dot structure the carbon domains are probably not nearly as uniform as a shell, and as a result the quenching effect by the embedded TiO$_2$ nanoparticles could be nearly quantitative for some parts of the carbon domains and not so much for other parts, with the observed lower fluorescence quantum yields representing averages for the samples.
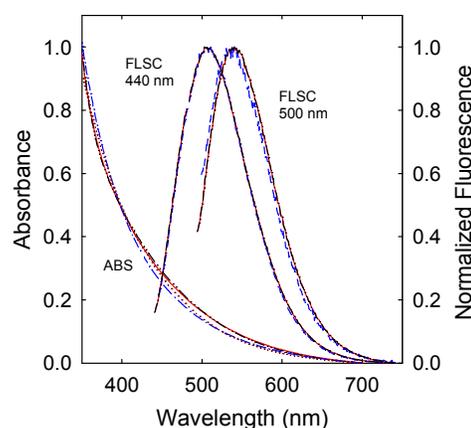

Figure 7. Absorption (ABS) and fluorescence (FLSC, with the excitation wavelengths shown) spectra of the C/TiO$_2$-Dots with 71 wt% (——) and 31 wt% (-..-..-) TiO$_2$, and the PEG-CDots (-.-.-). The absorption spectrum of the aqueous suspended small carbon nanoparticles (·······) is also shown for comparison.

The major difference in fluorescence performance between different arrangements of carbon and TiO$_2$ in the dots, the C$_{TiO2}$-Dots vs the C/TiO$_2$-Dots (Figure 1), may reflect the different functions of the TiO$_2$ in these hybrid nanostructures. In the former, the relatively small amount of TiO$_2$ on the surface of carbon nanoparticles (probably concentrated at the surface defect sites) serves the function of a "co-surface passivation agent" to enhance the passivation effect by the organic functionalization molecules, thus higher fluorescence quantum yields.[22,41] On the other hand, the TiO$_2$ nanoparticles in the C/TiO$_2$-Dots are conceptually and practically similar to those in the dye-sensitized TiO$_2$ systems,[45-48] serving as the recipient of the photon energies originally harvested by the dye sensitizer, here the carbon domains in the hybrid CDots.

Fluorescence decay results (Figure 8) suggest that the difference in decays among the different hybrid dots is much less significant than the difference in fluorescence quantum yields. Such an apparent decoupling between fluorescence lifetimes and quantum yields has been found in other CDots and dot configurations,[42,49,50] which has been explained in terms of essentially a three-state scheme with two excited state processes that are

fast (less than 100 ps) and slow (on the nanosecond time scale) and corresponding to yields Φ_1 and Φ_2, respectively.[42,50] The steady-state measurements for quantum yields may capture both processes, with observed fluorescence quantum yields $\Phi_F = \Phi_1\Phi_2$,[42,50] while time-resolved measurements on the nanosecond time scale (Figure 8) are limited only to the second process represented by Φ_2. The same mechanistic explanation may be applied to the apparent similarities in the excitation wavelength dependence of fluorescence spectra between the CDots without and with TiO$_2$ (Figure 2), suggesting that the excited state-ground state energy gaps associated with the Φ_2 process are not significantly affected by the presence of TiO$_2$.
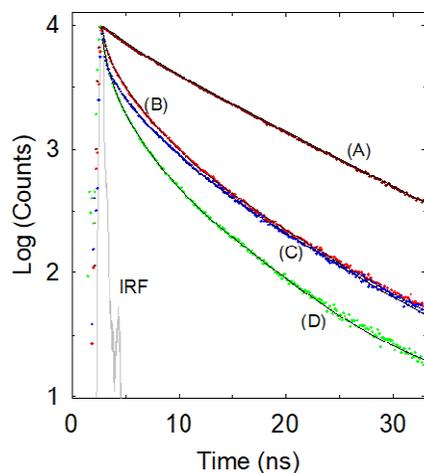

Figure 8. Fluorescence decay curves (440 nm excitation and 525 nm emission) and the deconvolution fits with a two-exponential function for the C$_{TiO2}$-Dots (A), PEG-CDots (B), and C/TiO$_2$-Dots with 31 wt% TiO$_2$ (C) and 71 wt% TiO$_2$ (D) in aqueous solutions. The fitting parameters are provided in the Electronic Supplementary Information.

CDots are known for their characteristic photoinduced redox properties, serving as both excellent electron acceptors and donors.[6,15] In this study, the hybrid dots and PEG-CDots were evaluated for their photoinduced electron transfer properties in fluorescence quenching experiments with *N,N*-diethylaniline (DEA) and 2,4-dinitrotoluene (DNT) as electron donating and accepting quenchers, respectively, in methanol solutions. As a reference, the fluorescence quenching results for the PEG-CDots (Figure 9, Table 1) are largely the same as those of other CDots in the literature,[6,50,51] as expected. Also might be expected are the fluorescence quenching results for the C$_{TiO2}$-Dots (Figure 9, Table 1), whose photoinduced electron transfer characteristics are similar to those of neat CDots without any TiO$_2$, as again the relatively small amount of TiO$_2$ serves only the function of enhancing surface passivation. With the estimated average fluorescence lifetimes $\tau_F°$ of 5.4 – 8.6 ns (Figure 8) for these dots, the Stern-Volmer constants (K_{SV}, Table 1) for DEA and DNT quenchers correspond to diffusion rate constants k_q ($K_{SV}/\tau_F°$) of 2.2×10^9 M^{-1}s^{-1} and larger (Table 1), suggesting diffusion control. However, despite their photoinduced redox characteristics of serving as both excellent electron acceptors and donors, CDots are generally much more effective in donating electrons.[15,50,51] Except for the C/TiO$_2$-Dots with 71 wt% TiO$_2$, the seemingly abnormally large k_q values (Table 1) beyond diffusion control for the quenching by DNT are rationalized as being due to a larger quenching radius than the dot radius when the dots are serving as electron donors,[50,51] demonstrating their extraordinary electron donating

ability. Such ability is apparently dampened by the substantial presence of TiO$_2$ in the C/TiO$_2$-Dots with the higher TiO$_2$ content (Figure 9, Table 1), probably due to the competing quenching effect by the embedded TiO$_2$.

The results presented and discussed above have demonstrated clearly that in the carbon hybrid dots with TiO$_2$, the structural configuration on the arrangement between the carbon and TiO$_2$ domains in the core nanoparticles of the dots plays a critical role in the dots' optical and photoinduced redox properties. Generally on carbon-TiO$_2$ hybrid nanostructures, one would expect their properties to be similar to those found in dye-sensitized TiO$_2$ systems,[45-48] namely for the carbon domains to serve the dye function of photon-harvesting in the visible spectral region where TiO$_2$ nanoparticles have no absorptions, and for the harvested photon energies to subsequently sensitize the TiO$_2$ in the hybrid dots. However, such an expectation is obviously not generally applicable to carbon-TiO$_2$ hybrid dots, again depending fundamentally on the configuration of the carbon and TiO$_2$ domains in the dots. In the C$_{TiO2}$-Dots, the small amount of TiO$_2$ coated/doped at the various surface sites of the carbon nanoparticles is likely insufficient in terms of quenching the photoexcited states of the carbon nanoparticles (or for their being sensitized if viewed from the opposite angle). Instead, the coated/doped TiO$_2$ is more likely a part of the surface passivation schemes for the carbon nanoparticles, in conjunction with the organic functional molecules, to result in much enhanced fluorescence emissions in the C$_{TiO2}$-Dots. Also consistent with the excited state properties are their redox characteristics as reflected in the redox quenching results. Thus, the C$_{TiO2}$-Dots may simply be considered as a class of high-performance CDots, though the mechanistic links between the participation of the TiO$_2$ in the surface passivation schemes and the obviously high performance of the resulting dots remain to be explored in further investigations.
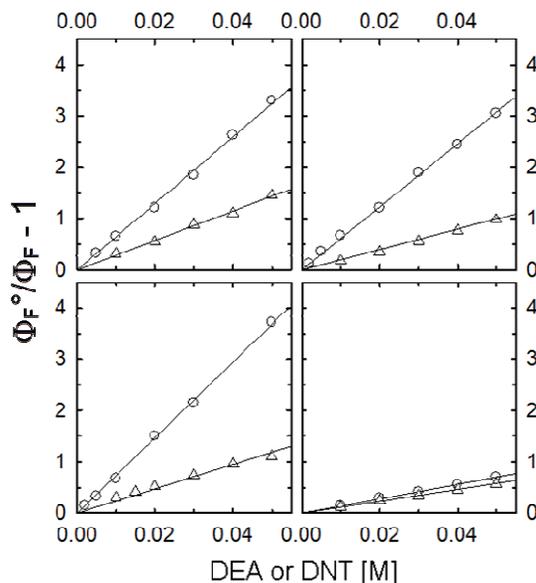

Figure 9. Stern-Volmer plots on the quenching of fluorescence quantum yields (440 nm excitation) by DEA (triangle) and DNT (circle) for the PEG CDots (upper left), C$_{TiO2}$-Dots (upper right), and C/TiO$_2$-Dots with 31 wt% TiO$_2$ (lower left) and 71 wt% TiO$_2$ (lower right) in methanol solutions.

Table 1. Quenching Results from Stern-Volmer Plots.

Dot Sample	K_{SV} (M^{-1})		k_q (M^{-1}s^{-1})	
	DNT	DEA	DNT	DEA
PEG-CDots	64	28	9.6×10^9	4.2×10^9
C$_{TiO2}$-Dots	68	21	7.9×10^9	2.4×10^9
C/TiO$_2$-Dots (31 wt% TiO$_2$)	67	22	9.5×10^9	3.1×10^9
C/TiO$_2$-Dots (71 wt% TiO$_2$)	14	12	2.6×10^9	2.2×10^9

In a structurally different or almost reversed configuration between the carbon and TiO$_2$ domains in core nanoparticles, with essentially TiO$_2$ nanoparticles coated with carbon domains in the C/TiO$_2$-Dots, there seems indeed the kind of behavior of dye-sensitized TiO$_2$ systems, especially when the TiO$_2$ content is higher. This is also supported by the results on the redox quenching of fluorescence emissions in these hybrid dots. Further investigations to look more closely into the functions of the sensitized TiO$_2$ (with the photon energies initially harvested by the carbon domains in the dots) will prove interesting and valuable to many related applications.

Conclusions

Carbon-TiO$_2$ hybrid dots in different structural configurations are apparently rather different in their optical properties and photoinduced redox characteristics. In the configuration of small carbon nanoparticles each coated/doped with only a small amount of TiO$_2$, the role of TiO$_2$ is simply a co-surface passivation "agent" and apparently an effective one. On the other hand, the hybrid dots of TiO$_2$ nanocrystals each composited with nanoscale carbon domains may be considered as being similar to dye-sensitized semiconductors, with the carbon domains serving the dye functions for the harvesting of visible photons, thus more relevant to various energy conversation uses. The results offer insights into the mechanistic relationships between the hybrid nano-structures/configurations and optical/redox properties, which should be valuable to the further exploration of carbon-metal oxide hybrid dots and their applications.

Experimental

Materials. The carbon nanopowder sample and *O,O'*-bis(3-aminopropyl) polyethylene glycol (PEG$_{1500N}$, average molecular weight ~1,500) were purchased from Aldrich. Nitric acid (60-70%), ethanol (>99%), sodium dodecyl sulfate (SDS, 99%) were obtained from VWR, Ti(OC$_2$H$_5$)$_4$ (>97%) from Alfa Aesar, and polyethylene glycol oligomers (PEG$_{1500}$, average molecular weight ~1,500) from Fluka. *N,N*-diethylaniline was acquired from Avocado, and 2,4-dinitrotoluene from TCI. Silicon carbide powders (120 Grit) were supplied by Panadyne Abrasives, and the dialysis membrane tubings (molecular weight cut-off ~500 and ~2,000) by Spectrum Laboratories. Water was deionized and purified by being passed through a Labconco WaterPros water purification system.

Measurement. UV/vis absorption spectra were recorded on a Shimadzu UV2501-PC spectrophotometer. Fluorescence spectra were collected on a Horiba Jobin-Yvon emission spectrometer equipped with a 450 W xenon source, Gemini-180 excitation and Triax-550 emission monochromators, and a photon counting detector (Hamamatsu R928P PMT at 950 V). Fluorescence quantum yields were calculated against 9,10-bis(phenylethynyl)-anthracene in hexane as standard. Fluorescence decays were measured by time-correlated single photon counting (TCSPC) technique on a Horiba Ultima Extreme spectrometer equipped with a SuperK Extreme supercontinuum laser source pulsed at 10 MHz, TDM-800 excitation and TDM-1200 emission monochromators, a R3809-50 MCP-PMT detector operated at 3.0 kV in a thermoelectrically cooled housing, and FluoroHub A+ timing electronics. FT-IR spectra were obtained on a Shimadzu IRAffinity-1S spectrophotometer equipped with the Single Reflection ATR accessory for solid samples. Powder X-ray diffraction measurements were performed on a Rigaku Ultima IV X-ray diffractometer with Cu Kα radiation (λ = 1.5418 Å) at 25 °C. Transmission electron microscopy (TEM) images were acquired on a Hitachi H-9500 high-resolution TEM system and a Hitachi HD-2000 S-TEM system. The latter was also used for the in-situ energy dispersive X-ray spectroscopy (EDS) analysis. The TEM specimen was prepared by depositing a few drops of a dilute sample solution onto silicon-based grids, followed by the removal of solvent via evaporation. The thermogravimetric analysis (TGA) was performed on a TA Instruments Q600 machine. The inductively coupled plasma mass spectrometry (ICP-MS) analysis of titanium was on a Thermo Scientific X series II instrument.

C$_{TiO2}$-Dots. The as-supplied carbon nanopowders (1 g) were refluxed in an aqueous nitric acid solution (5 M, 100 mL) for 24 h. After being cooled to ambient temperature, the strongly acidic suspension was centrifuged at 1,000 *g* to retain the supernatant, and dialyzed (molecular weight cut-off ~500) against fresh water. The resulting aqueous suspension was evaporated to remove water to obtain the surface-oxidized carbon nanoparticles.

A clear solution of Ti(OC$_2$H$_5$)$_4$ (2.868 g) in a mixture of ethanol (51 mL), water (0.43 mL), and nitric acid (0.16 mL) was prepared. To an aliquot (50 mL) of the solution was added the treated carbon nanoparticles (200 mg), and the mixture was sonicated for 1 h, stirred for 12 h, and then filtrated. The filter cake was grounded and annealed at 250 °C for 1 h to obtain a solid sample. A portion (50 mg) of the sample was dispersed in an aqueous SDS solution (1 wt%, 120 mL) under sonication for 30 min, followed by filtration. The filter cake was washed with water several times, and then dried. The solid sample thus obtained was mixed well with PEG$_{1500N}$ (1 g), and the mixture was heated to 110 °C and stirred at the temperature for 72 h under nitrogen protection. The reaction mixture was cooled back to ambient temperature, and dispersed in water (15 mL). The dispersion was centrifuged at 20,000 *g* to retain the supernatant as an aqueous solution of the C$_{TiO2}$-Dots.[22]

C/TiO$_2$-Dots. Ti(OC$_2$H$_5$)$_4$ (2.868g), ethanol (51 mL), water (0.43 mL), and nitric acid (0.16 mL) were mixed, and the mixture was transferred to a Teflon-lined autoclave for the treatment at 180 °C for 12 h. Upon being cooled back to ambient temperature, the milky reaction mixture was washed with ethanol and H$_2$O three times to obtain the TiO$_2$ nanoparticles.

The TiO$_2$ nanoparticles were dispersed in ethanol, and the dispersion was mixed well with the oligomeric PEG$_{1500}$ under sonication, followed by nitrogen purging to remove the ethanol. The resulting solid-state mixture in a glass vial was immersed in a silicon carbide bath (about 8 cm in diameter and 2.5 cm in height, containing about 50 g silicon carbide) for thermal treatment in a conventional microwave oven at 1,000 W. The degree of carbonization and thus the carbon content in the core carbon nanoparticles of the hybrid dots (excluding the carbons in the surface PEG moieties) was varied by adjusting the TiO$_2$/PEG$_{1500}$ ratio in the precursor mixture for the

microwave treatment and the treatment time. Specifically, a mixture of TiO_2 (40 mg) and PEG_{1500} (1 g) was treated with microwave irradiation at 1,000 W for 7 min. The reaction mixture was cooled to ambient temperature and dispersed in deionized water (10 mL), followed by dialysis (molecular weight cut-off ~2,000) against fresh water to obtain the C/TiO_2-Dots of 29 wt% carbon and 71 wt% TiO_2. In a somewhat different procedure, a mixture of TiO_2 (40 mg) and PEG_{1500} (2 g) was treated with microwave irradiation at 1,000 W for 12 min, followed by allowing the sample to cool down, and then further microwave irradiation at 1,000 W for 12 min. The sample was dispersed in deionized water (10 mL), and similarly dialyzed to obtain the C/TiO_2-Dots of 69 wt% carbon and 31 wt% TiO_2. The carbon contents in the core carbon nanoparticles of the dots were estimated by TGA with the experimental condition of first heating to 600 °C at a rate of 10 °C/min in nitrogen flow, holding the temperature constant at 600 °C for 30 min in air flow, and then heating to 800 °C again at a rate of 10 °C/min.

## Conflicts of interest

There are no conflicts to declare.

Acknowledgements

Notes and references

1   Y.-P. Sun, B. Zhou, Y. Lin, W. Wang, sK. A. S. Fernando, P. Pathak, M. J. Meziani, B. A. Harruff, X. Wang, H. Wang, P. G. Luo, H. Yang, M. E. Kose, B. Chen, L. M. Veca and S.-Y. Xie, Quantum-Sized Carbon Dots for Bright and Colorful Photoluminescence. *J. Am. Chem. Soc.* **2006**, *128*, 7756-7757.

2   Y.-P. Sun. Fluorescent Carbon Nanoparticles, U.S. Patent 7,829,772, **2006**.

3   L. Cao, X. Wang, M. J. Meziani, F. Lu, H. Wang, P. G.. Lin, B. A. Harruff, L. M. Veca, D. Murray, S.-Y. Xie and Y.-P. Sun, Carbon Dots for Multiphoton Bioimaging. *J. Am. Chem. Soc.* **2007**, *129*, 11318-11319.

4   X. Wang, L. Cao, S.-T. Yang, F. Lu, M. J. Meziani, L. Tian, K. W. Sun, M. A. Bloodgood and Y.-P. Sun, Bandgap-Like Strong Fluorescence in Functionalized Carbon Nanoparticles. *Angew. Chem. Int. Ed.* **2010**, *49*, 5310-5314.

5   X. Hou, Y. Hu, P. Wang, L. Yang, M. M. Al Awak, Y. Tang, F. K.Twara, H. Qian and Y.-P. Sun, Modified Facile Synthesis for Quantitatively Fluorescent Carbon Dots. *Carbon* **2017**, *122*, 389-394.

6   X. Wang, L. Cao, F. Lu, M. J. Meziani, H. Li, G. Qi, B. Zhou, B. A. Harruff, F. Kermarrec and Y.-P. Sun, Photoinduced Electron Transfers with Carbon Dots. *Chem. Commun.* **2009**, 3774-3776.

7   L. Cao, S. Sahu, P. Anilkumar, C. E. Bunker, J. Xu, K. A. S. Fernando, P. Wang, E. A. Guliants, K. N. Tackett, II and Y.-P. Sun, Carbon Nanoparticles as Visible-Light Photocatalysts for Efficient CO_2 Conversion and Beyond. *J. Am. Chem. Soc.* **2011**, *133*, 4754-4757.

8   Z. Zhang, T. Zheng, X. Li, J. Xu and H. Zeng, Progress of Carbon Quantum Dots in Photocatalysis Applications. *Part. Part. Syst. Char.* **2016**, *33*, 457-472.

9   P. Juzenas, A. Kleinauskas, P. G. Luo and Y.-P. Sun, Photoactivatable Carbon Nanodots for Cancer Therapy. *Appl. Phys. Lett.* **2013**, *103*, 063701.

10 Y. Choi, S. Kim, M.-H. Choi, S.-R. Ryoo, J. Park, D.-H. Min and B.-S. Kim, Biocompatible Carbon Nanodots for Simultaneous Bioimaging and Targeted Photodynamic Therapy in Vitro and in Vivo. *Adv. Funct. Mater.* **2014**, *24*, 5781-5789.

11 M. J. Meziani, X. Dong, L. Zhu, L. P. Jones, G. E. LeCroy, F. Yang, S. Wang, P. Wang, Y. Zhao, L. Yang, R. A. Tripp and Y.-P. Sun, Visible-Light-Activated Bactericidal Functions of Carbon "Quantum" Dots. *ACS Appl. Mater. Interfaces* **2016**, *8*, 10761-10766.

12 P. G. Luo, S. Sahu, S.-T. Yang, S. K. Sonkar, J. Wang, H. Wang, G. E. LeCroy, L. Cao and Y.-P. Sun, Carbon "Quantum" Dots for Optical Bioimaging. *J. Mater. Chem. B* **2013**, *1*, 2116-2127.

13 P. Roy, P. C. Chen, A. P. Periasamy, Y. N. Chen and H. T. Chang, Photoluminescent Carbon Nanodots: Synthesis, Physicochemical Properties and Analytical Applications. *Mater. Today* **2015**, *18*, 447-458.

14 S. Y. Lim, W. Shen and Z. Gao, Carbon Quantum Dots and Their Applications. *Chem. Soc. Rev.* **2015**, *44*, 362-381.

15 K. A. S. Fernando, S. Sahu, Y. Liu, W. K. Lewis, E. A. Guliants, A. Jafariyan, P. Wang, C. E. Bunker and Y.-P. Sun, Carbon Quantum Dots and Applications in Photocatalytic Energy Conversion. *ACS Appl. Mater. Interfaces* **2015**, *7*, 8363-8376.

16 G. E. LeCroy, S. T. Yang, F. Yang, Y. M. Liu, K. A. S. Fernando, C. E. Bunker, Y. Hu, P. G. Luo and Y.-P. Sun, Functionalized Carbon Nanoparticles: Syntheses and Applications in Optical Bioimaging and Energy Conversion. *Coord. Chem. Rev.* **2016**, *320*, 66-81.

17 X. Sun, and Y. Lei, Fluorescent Carbon Dots and Their Sensing Applications. *Trends Anal. Chem.* **2017**, *89*, 163-180.

18 R. Wang, K.-Q. Lu, Z.-R. Tang and Y.-J. Xu, Recent Progress in Carbon Quantum Dots: Synthesis, Properties and Applications in Photocatalysis. *J. Mater. Chem. A* **2017**, *5*, 3717-3734.

19 J. Wang, H. S. Choi, Y.-X. and J. Wang, Exponential Growth of Publications on Carbon Nanodots by Chinese Authors. *J. Thorac. Dis.* **2015**, *7*, E201-E205.

20 Z. Zhou, Y. Shen, Y. Li, A. Liu, S. Liu, and Y. Zhang, Chemical Cleavage of Layered Carbon Nitride with Enhanced Photoluminescent Performances and Photoconduction. *ACS Nano*, **2015**, *9*, 12480-12487.

21 Y. Zhang and A. Markus, Photocurrent Generation by Polymeric Carbon Nitride Solids: An Initial Step towards a Novel Photovoltaic System. *Chem. Asian J.*, **2010**, 5, 1307-1311.

22 P. Anilkumar, X. Wang, L. Cao, S. Sahu, J.-H. Liu, P. Wang, K. Korch, K. N. Tackett, II, A. Parenzan and Y.-P. Sun, Toward Quantitatively Fluorescent Carbon-Based "Quantum" Dots. *Nanoscale* **2011**, *3*, 2023-2027.

23 G. E. LeCroy, S. K. Sonkar, F. Yang, L. M. Veca, P. Wang, K. N. Tackett, II, J.-J. Yu, E. Vasile, H. Qian, Y. Liu, P. G. Luo and Y.-P. Sun, Toward Structurally Defined Carbon Dots as Ultracompact Fluorescent Probes. *ACS Nano* **2014**, *8*, 4522-4529.

24 A. Jaiswal, S. S. Ghosh and A. Chattopadhyay, One Step Synthesis of C-Dots by Microwave Mediated Caramelization of Poly(Ethylene Glycol). *Chem. Commun.* **2012**, *48*, 407-409.

25 Y. Yang, J. Cui, M. Zheng, C. Hu, S. Tan, Y. Xiao, Q. Yang and Y. Liu, One-Step Synthesis of Amino-Functionalized Fluorescent Carbon Nanoparticles by Hydrothermal Carbonization of Chitosan. *Chem. Commun.* **2012**, *48*, 380-382.

26 Y. Wang and A. Hu. Carbon Quantum Dots: Synthesis, Properties and Applications. *J. Mater. Chem. C* **2014**, *2*, 6921-6939.

27 R. Liu, H. Huang, H. Li, Y. Liu, J. Zhong, Y. Li, S. Zhang and Z. Kang, Metal Nanoparticle/Carbon Quantum Dot Composite as a Photocatalyst for High-Efficiency Cyclohexane Oxidation. *ACS Catalysis* **2013**, *4*, 328-336.

28 H. Wang, Z. Wei, H. Matsui and S. Zhou, Fe_3O_4/Carbon Quantum Dots Hybrid Nanoflowers for Highly Active and Recyclable Visible-Light Driven Photocatalyst. *J. Mater. Chem. A* **2014**, *2*, 15740-15745.

29 H. Li, X. Zhang and D. R. MacFarlane, Carbon Quantum Dots/Cu_2O Heterostructures for Solar-Light-Driven Conversion of CO_2 to Methanol. *Adv. Energy Mater.* **2015**, *5*, 1401077.

30 B. De and N. Karak, Recent Progress in Carbon Dot–Metal Based Nanohybrids for Photochemical and Electrochemical Applications. *J. Mater. Chem. A* **2017**, *5*, 1826-1859.

31 Y. Hu, P. Wang, C. E. Bunker, L. R. Teisl, M. Reibold, S. Yan, H. Qian, D. He and Y.-P. Sun, Preparation and Optical Properties of Magnetic Carbon/Iron Oxide Hybrid Dots. *RSC Adv.*, **2017**, *7*, 41304-41310.

32 A. Zana, C. Rüdiger, J. Kunze-Liebhäuser, G. Granozzi, N. E. A. Reeler, T. Vosch, J. J. K. Kirkensgaard and M. Arenz, Core-Shell TiO_2@C: Towards Alternative Supports as Replacement for High Surface Area Carbon for Pemfc Catalysts. *Electrochim. Acta* **2014**, *139*, 21-28.

33 J. Liu, W. Zhu, S. Yu and X. Yan, Three Dimensional Carbogenic Dots/TiO_2 Nanoheterojunctions with Enhanced Visible Light-Driven Photocatalytic Activity. *Carbon* **2014**, *79*, 369-379.

34 W. Zhang, X. Zhang, Z. Zhang, W. Wang, A. Xie, C. Xiao, H. Zhang and Y. Shen, A Nitrogen-Doped Carbon Dot-Sensitized TiO_2 Inverse Opal Film: Preparation, Enhanced Photoelectrochemical and Photocatalytic Performance. *J. Electrochem. Soc.* **2015**, *162*, H638-H644.

35 M. Vasei, P. Das, H. Cherfouth, B. Marsan and J. P. Claverie, TiO_2@C Core-Shell Nanoparticles Formed by Polymeric Nano-Encapsulation. *Front. Chem.* **2014**, *2*, 47.

36 J. Wang, M. M. Gao and G. W. Ho, Bidentate-Complex-Derived TiO_2/Carbon Dot Photocatalysts: In Situ Synthesis, Versatile Heterostructures, and Enhanced H_2 Evolution. *J. Mater. Chem. A* **2014**, *2*, 5703-5709.

37 B. Sambandam, A. Surenjan, L. Philip and T. Pradeep, Rapid Synthesis of C-TiO_2: Tuning the Shape from Spherical to Rice Grain Morphology for Visible Light Photocatalytic Application. *ACS Sustain. Chem. Eng.* **2015**, *3*, 1321-1329.

38 S. Sahu, Y. Liu, P. Wang, C. E. Bunker, K. A. S. Fernando, W. K. Lewis, E. A. Guliants, F. Yang, J. Wang and Y.-P. Sun, Visible-Light Photoconversion of Carbon Dioxide into Organic Acids in an Aqueous Solution of Carbon Dots. *Langmuir* **2014**, *30*, 8631-8636.

39 S. Xie, H. Su, W. Wei, M. Li, Y. Tong and Z. Mao, Remarkable Photoelectrochemical Performance of Carbon Dots Sensitized TiO_2 under Visible Light Irradiation. *J. Mater. Chem. A* **2014**, *2*, 16365-16368.

40 Y.-Q. Zhang, D.-K. Ma, Y.-G. Zhang, W. Chen and S.-M. Huang, N-Doped Carbon Quantum Dots for TiO_2-Based Photocatalysts and Dye-Sensitized Solar Cells. *Nano Energy* **2013**, *2*, 545-552.

41 Y.-P. Sun, X. Wang, F. Lu, L. Cao, M. J. Meziani, P. G. Luo, L. Gu and L. M. Veca, Doped Carbon Nanoparticles as a New Platform for Highly Photoluminescent Dots. *J. Phys. Chem. C* **2008**, *112*, 18295-18298.

42 F. Yang, G. E. LeCroy, P. Wang, W. Liang, J. Chen, K. A. S. Fernando, C. E. Bunker, H. Qian and Y.-P. Sun, Functionalization of Carbon Nanoparticles and Defunctionalization–Toward Structural and Mechanistic Elucidation of Carbon "Quantum" Dots. *J. Phys. Chem. C* **2016**, *120*, 25604-25611.

43 A. Jitianu, T. Cacciaguerra, R. Benoit, S. Delpeux, F. Béguin and S. Bonnamy, Synthesis and Characterization of Carbon Nanotubes-TiO_2 Nanocomposites. *Carbon* **2004**, *42*, 1147-1151.

44 H. M. Yadav and J.-S. Kim, Solvothermal Synthesis of Anatase TiO_2-Graphene Oxide Nanocomposites and Their Photocatalytic Performance. *J. Alloys Compd.* **2016**, *688*, 123-129.

45 C. Chen, W. Ma and J. Zhao, Semiconductor-Mediated Photodegradation of Pollutants under Visible-Light Irradiation. *Chem. Soc. Rev.* **2010**, *39*, 4206-4219.

46 J. H. Bang and P. V. Kamat, Solar Cells by Design: Photoelectrochemistry of TiO_2 Nanorod Arrays Decorated with CdSe. *Adv. Funct. Mater.* **2010**, *20*, 1970-1976.

47 J. Gong, K. Sumathy, Q. Qiao and Z. Zhou, Review on Dye-Sensitized Solar Cells (Dsscs): Advanced Techniques and Research Trends. *Renew. Sustain. Energy Rev.* **2017**, *68*, 234-246.

48 M. Ge, Q. Li, C. Cao, J. Huang, S. Li, S. Zhang, Z. Chen, K. Zhang, S. S. Al-Deyab and Y. Lai, One-Dimensional TiO_2 Nanotube Photocatalysts for Solar Water Splitting. *Adv. Sci.* **2017**, *4*, 1600152.

49 Y. Liu, P. Wang, K. A. S. Fernando, G. E. LeCroy, H. Maimaiti, B. A. Harruff-Miller, W. K. Lewis, C. E. Bunker, Z.-L. Hou and Y.-P. Sun, Enhanced Fluorescence Properties of Carbon Dots in Polymer Films. *J. Mater. Chem. C* **2016**, *4*, 6967-6974.

50 G. E. LeCroy, F. Messina, A. Sciortino, C. E. Bunker, P. Wang, K. A. S. Fernando and Y.-P. Sun, Characteristic Excitation Wavelength Dependence of Fluorescence Emissions in Carbon "Quantum" Dots. *J. Phys. Chem. C* **2017**, *121*, 28180-28186.

51 G. E. LeCroy, K. A. S. Fernando, C. E. Bunker, P. Wang, N. Tomlinson and Y.-P. Sun, Steady-State and Time-Resolved Fluorescence Studies on Interactions of Carbon "Quantum" Dots with Nitrotoluenes. *Inorg. Chim. Acta* **2017**, *468*, 300-307.
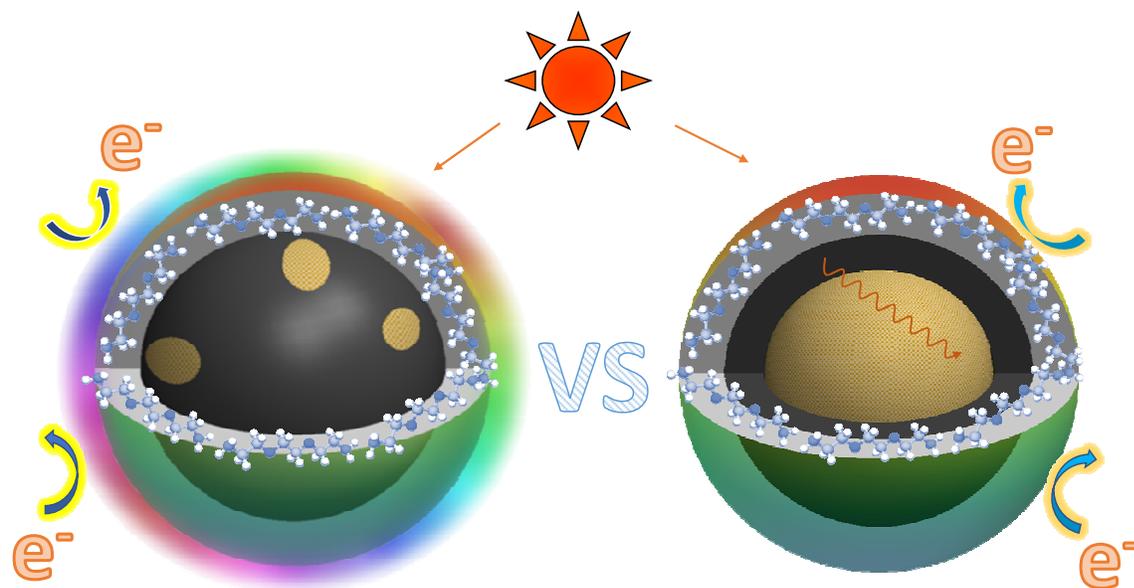
Carbon-TiO$_2$ hybrid dots in different structural configurations were found to exhibit very different optical properties and photoinduced redox characteristics.